ELSEVIER

Journal of Power Sources 110 (2002) 437–444

JOURNAL OF POWER SOURCES

www.elsevier.com/locate/jpowsour

# Design modeling of lithium-ion battery performance

Paul Nelson*, Ira Bloom, Khalil Amine, Gary Henriksen

*Electrochemical Technology Program, Argonne National Laboratory, Bldg. 205, 9700 South Cass Avenue, Argonne, IL 60439, USA*

**Abstract**

A computer design modeling technique has been developed for lithium-ion batteries to assist in setting goals for cell components, assessing materials requirements, and evaluating thermal management strategies. In this study, the input data for the model included design criteria from Quallion, LLC for Gen-2 18650 cells, which were used to test the accuracy of the dimensional modeling. Performance measurements on these cells were done at the electrochemical analysis and diagnostics laboratory (EADL) at Argonne National Laboratory. The impedance and capacity related criteria were calculated from the EADL measurements. Five batteries were designed for which the number of windings around the cell core was increased for each succeeding battery to study the effect of this variable upon the dimensions, weight, and performance of the batteries. The lumped-parameter battery model values were calculated for these batteries from the laboratory results, with adjustments for the current collection resistance calculated for the individual batteries.


*Keywords:* Lithium-ion; Battery modeling; Cell testing; Lumped-parameter model; PNGV battery; Hybrid electric vehicle

## 1. Introduction

The partnership for a new generation of vehicles (PNGV) was established between the US government and the US council for automotive research (USCAR) in 1993 to develop new fuel-efficient automobiles. Hybrid electric vehicles (HEVs), which have a small engine and one or more battery-powered motors to boost acceleration power, are under development for PNGV. The drive trains of these HEVs are fuel-efficient for several reasons. The engine is smaller, and therefore, more efficient than that of a conventional vehicle with the same total power. The engine of the HEV is operated under conditions where it is efficient, which are at high power for acceleration and for recharging the battery. The battery and electric motor provide the power at low power demand, where energy efficiency would be poor for the engine. Energy from braking the vehicle, which is dissipated as heat in conventional mechanical braking systems, is charged into the HEV battery for reuse.

The requirements for an HEV battery for the PNGV program are very demanding, as shown in Table 1 from [1]. There are two types of HEVs under study: the power-assist HEV, which uses a battery-powered motor on rapid accelerations to assist the engine, and the dual-mode HEV, which is designed to operate under battery power alone for several miles of travel.

In this effort, we have studied the performance of batteries in the power-assist HEV. Batteries for the vehicles were designed with the use of a computer design program. Part of the input to the program was experimental data on lithium-ion cells under development for PNGV.

## 2. Modeling and testing of 18650 cells

The batteries designed for this study are based on the lithium-ion system being studied by the US department of energy (DOE) in the advanced technology development (ATD) program. The compositions of the materials in this system have been designated Gen-2 and consist of a positive electrode material of $LiNi_{0.8}Al_{0.05}Co_{0.15}O_2$ (8% PVDF binder, 4% SFG-6 graphite, 4% carbon black) and a negative electrode of MAG-10 graphite (8% PVDF binder) with an electrolyte of 1.2 M $LiPF_6$ in EC:EMC (3:7) and 25 μm thick PE Celgard separators. Quallion, LLC has fabricated 165 cells of the 18650 size with electrodes of this composition for testing at Argonne National Laboratory, Idaho National Engineering Laboratory, and Sandia National Laboratory. Similar tests had been carried out by these laboratories on 18650 cells made with a Gen-1 cell composition [2].

### 2.1. Model verification

To achieve the high power required for the PNGV application, the electrodes were made very thin (35 μm) and

* Corresponding author.
*E-mail address:* nelson@cmt.anl.gov (P. Nelson).

0378-7753/02/$ – see front matter © 2002 Published by Elsevier Science B.V.
PII: S0378-7753(02)00209-4

Table 1
PNGV energy storage system performance goals

| Characteristics | Units | Power-assist | Dual-mode |
|---|---|---|---|
| Pulse discharge power | kW | 25 (18 s) | 45 (12 s) |
| Peak regenerative pulse power | kW | 30 (2 s)<br>(min 50 Wh over 10 s regen total) | 35 (10 s)<br>(97 Wh pulse) |
| Total available energy (over DOD range where power goals are met) | kWh | 0.3 (at 1 C rate) | 1.5 (at 6-kW constant power) |
| Minimum round-trip energy efficiency | % | 90 | 88 |
| Cold cranking power at −30 °C (three 2 s pulses, 10 s resets between) | kW | 5 | 5 |
| Cycle-life, for specified SOC increments | Cycles | 300,000<br>Power-assist cycles (7.5 MWh) | 3750<br>Dual-mode cycles (22.5 MWh) |
| Calendar life | Years | 15 | 15 |
| Maximum weight | kg | 40 | 100 |
| Maximum volume | l | 32 | 75 (at 165 mm max height) |
| Operating voltage limits (note: maximum current is limited to 217 A at any power level) | Vdc | Max <440 min >(0.55 x Vmax) | Max <440 min >(0.5 x Vmax) |
| Maximum allowable self-discharge rate | Wh per day | 50 | 50 |
| Temperature range | | | |
| Equipment operation | °C | −30 to + 52 | −30 to + 52 |
| Equipment survival | | −46 to + 66 | −46 to + 66 |

coated on both sides of the current collector foils (30 μm aluminum for the positive electrode and 18 μm copper for the negative electrode). These electrodes and 25 μm Celgard separators were wound around a polymer core to fabricate the 18650 cells. Quallion, LLC provided proprietary data on the dimensions of the cell winding materials and the weights of cell components to ANL for design and modeling studies.

ANL prepared a spreadsheet model to design cells, which was verified by comparing the calculated parameters for an 18650 cell with the information from Quallion, LLC (Table 2).

## 2.2. Cell testing

Tests were conducted on 18650 cells at ANL to determine the cell capacity for a discharge and charge at the 1 C rate. The discharge–charge curves are shown in Fig. 1. The open-circuit

Table 2
Agreement between measured dimensions and weights of lithium-ion 18650 cells and values calculated by modeling

| | Error in calculated value (%) |
|---|---|
| Lengths of winding materials (mm) | |
| Positive electrode | 0.1 |
| Negative electrode | −0.8 |
| Separators | 1.2 |
| Cell area ($cm^2$) | 0.2 |
| Weights (g)[a] | |
| Positive electrode | 1.0 |
| Negative electrode | 1.6 |
| Electrolyte | −0.4 |
| Balance of cell | 2.3 |
| Total | 1.0 |

[a] Measured weights are averages for 17 randomly selected cells.

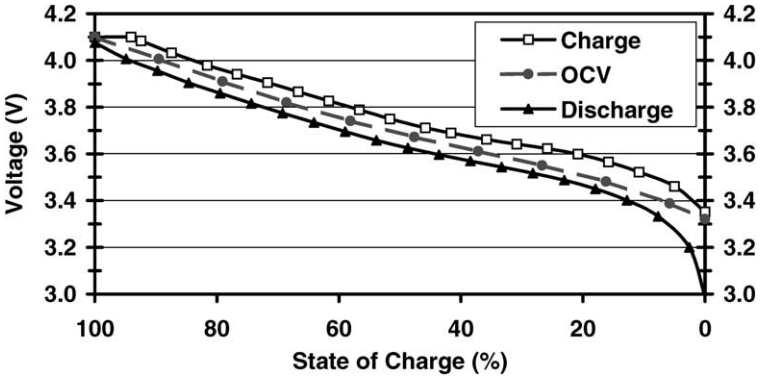


Fig. 1. Charge and discharge at the 1 C rate for 18650 cells of Gen-2 composition.

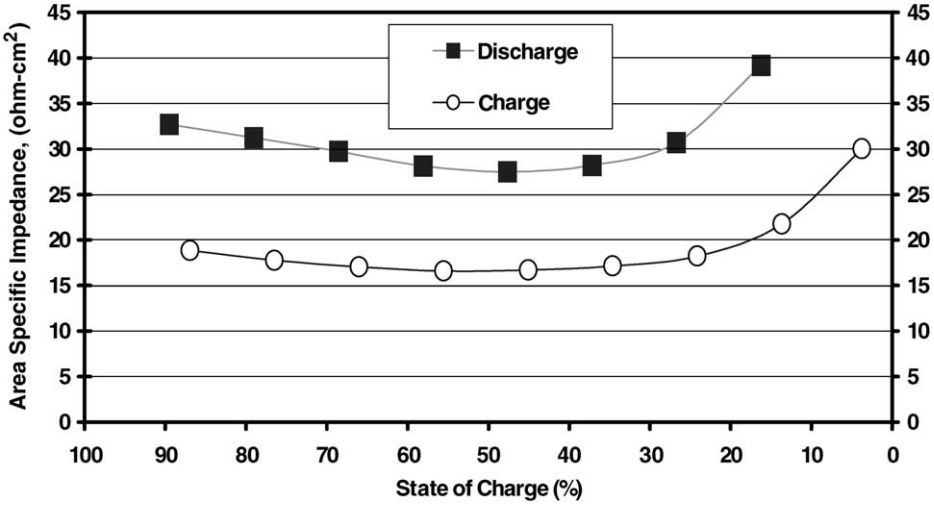


Fig. 2. Impedance of Gen-2 18650 cells for 18 s discharges and 2 s charges as a function of state of charge.

voltage (OCV) curve is also shown in this figure. In other runs we conducted hybrid pulse power characterization (HPPC) tests according to the procedures described in [1]. In these tests, the cell discharge power at the end of an 18 s pulse and the regeneration power at the end of a 2 s pulse are determined as a function of depth of discharge. The cells are discharged at the 1 C rate and the pulse power tests are made at 10% state-of-charge (SOC) intervals after a 1 h rest period to establish the OCV. The area-specific impedance (ASI) values obtained in these tests for a typical cell, with the calculated resistance of the current collection system subtracted, are shown in Fig. 2. The impedance changes little in the middle of the SOC range.

An accurate estimation curve for the OCV was obtained from the HPPC measurements by correlating the data on OCV, V obtained for the SOC range of 16.2–79%.

$$\mathrm{OCV} = ax^4 + bx^3 + cx^2 + dx + e \tag{1}$$

where $x = \%$ SOC/100; $a = -6.052$; $b = 12.554$; $c = -8.815$; $d = 3.0565$; $e = 3.1655$.

This curve reproduces the data to within 1.0 mV over the range of the correlation.

### 2.3. Lumped-parameter battery model

The measured cell voltages in the HPPC tests were subtracted from the OCV and this difference was correlated by means of a modification in the lumped-parameter battery model described in the PNGV Battery Test Manual [3]. The estimated voltage equation is the following:

$$\mathrm{OCV} - V_\mathrm{l} = R_\mathrm{o} I_\mathrm{l} + R_\mathrm{p} I_\mathrm{p} \tag{2}$$

where OCV = estimated OCV from Eq. (1); $V_\mathrm{l}$ = cell voltage, (V); $R_\mathrm{p}$ = cell internal "ohmic" resistance, (Ω); $R_\mathrm{p}$ = cell internal "polarization" resistance, (Ω); $I_\mathrm{l}$ = cell load current, (A); $I_\mathrm{p}$ = current through polarization resistance, (A).

$I_\mathrm{p}$ is derived from the differential equation:

$$\frac{\mathrm{d}I_\mathrm{p}}{\mathrm{d}t} = \frac{(I_\mathrm{l} - I_\mathrm{p})}{\tau} \tag{3}$$

For a time interval $\Delta t = t_\mathrm{i} - t_{\mathrm{i}-1}$, and a polarization time constant, $\tau$ in seconds, polarization current in amperes, $I_\mathrm{p}$, can be calculated at time, $t_\mathrm{i}$, by integration of Eq. (3).

Voltage and current measurements were available from the HPPC tests from which the ASI values were calculated for Fig. 2. From these measurements, the voltage difference OCV-$V_\mathrm{l}$ was correlated over the SOC range 58.1–37.2%, which includes three pulse discharges and charges and extended over 8000 s in intervals of 0.1–30 s, depending on the rate of change of current and voltage. The correlation was done with the EXCEL-based parameter estimation procedure with the residual value set to zero. The results are shown in Table 3 and Fig. 3. The correlation coefficient, $r^2$, was optimized at 0.997 when $\tau$ was set at 27 s. Fig. 3 shows only a 200 s section of the 8000 s period over which the data were correlated and only a few of the voltage measurements are shown for clarity. The estimated voltage fit the data about equally well over the entire 8000 s period. In Table 3, the value of $R_\mathrm{o}$ is shown as determined from the data on the 18650 cell and for this parameter with the calculated resistance of the current collector subtracted from $R_\mathrm{o}$. In applying Eq. (2) to calculate the impedance of a cell of the same material compositions and thickness but of different area and design, the resistance of the current collection system of that cell must be added to this adjusted value of $R_\mathrm{o}$.

## 3. Battery modeling

We developed a spreadsheet model for designing batteries comprised of flat-wound cells. The modeling program designs a cell and calculates the weight, volume, and electrical performance of all components and of the total

Table 3
Modeling of 18650 cells with lithium-ion electrodes measured and calculated performance

| | Measured | Calculated |
|---|---|---|
| Power related | | |
| Measured cell discharge impedance at 47.6% SOC (mohms) | 35 | |
| Measured cell charge impedance at 45.1% SOC (mohms) | 21 | |
| Current collection resistance (mohms) | | 0.651 |
| Percent of total discharge impedance | | 1.9 |
| Discharge impedance minus current collection (ohm $cm^2$) | | 29.1 |
| Charge impedance minus current collection (ohm $cm^2$) | | 17.2 |
| Lumped-parameter battery model | | |
| SOC range | | 58.1–37.2% |
| Correlation coefficient, $r^2$ | | 0.997 |
| Polarization time constant (τ), (s) | | 27 |
| Cell internal "ohmic" resistance $R_o$ (ohms) | | 0.01907 |
| Ohmic resistance less collection resistance (ohms) | | 0.01842 |
| Cell internal "polarization" resistance $R_p$ (ohms) | | 0.02388 |
| Energy related | | |
| Capacity at 1 C rate (Ah) | 0.978 | |
| Capacity density of positive material (mAh/g) | | 159 |
| Energy at 1 C rate (Wh) | 3.702 | |
| Average voltage on discharge (V) | | 3.650 |
| Average voltage corrected for collection losses | | 3.651 |
| Open-circuit voltage at 50% DOD (V) | | 3.671 |

cell with a selection of a large number of components. It also designs a battery for the PNGV application and calculates the weight, volume, power, available energy and operating voltage range. Cells and batteries of various combinations of dimensions can be designed to meet the overall PNGV criteria.

The compositions and thickness of the layered structures were the same as those in the 18650 cells discussed above. In this design study, batteries were designed to meet the PNGV program requirements for the power-assist vehicle battery. The spreadsheet program designs five batteries simultaneously with cells of the configuration shown in Fig. 4. The cell design for these batteries is based on winding the electrodes and separators around a core consisting of a polymer sleeve 0.5 mm thick and 4 mm across. The ample cross-section facilitates winding without breaking the electrode coatings and the hollow core is a reservoir for electrolyte. To achieve the high power required by the PNGV application, current has to be efficiently collected from each wrap of current collector foil. The proposed method for attaching the current collector foils to the terminal is gather the foils on one side of the core and weld them in a single

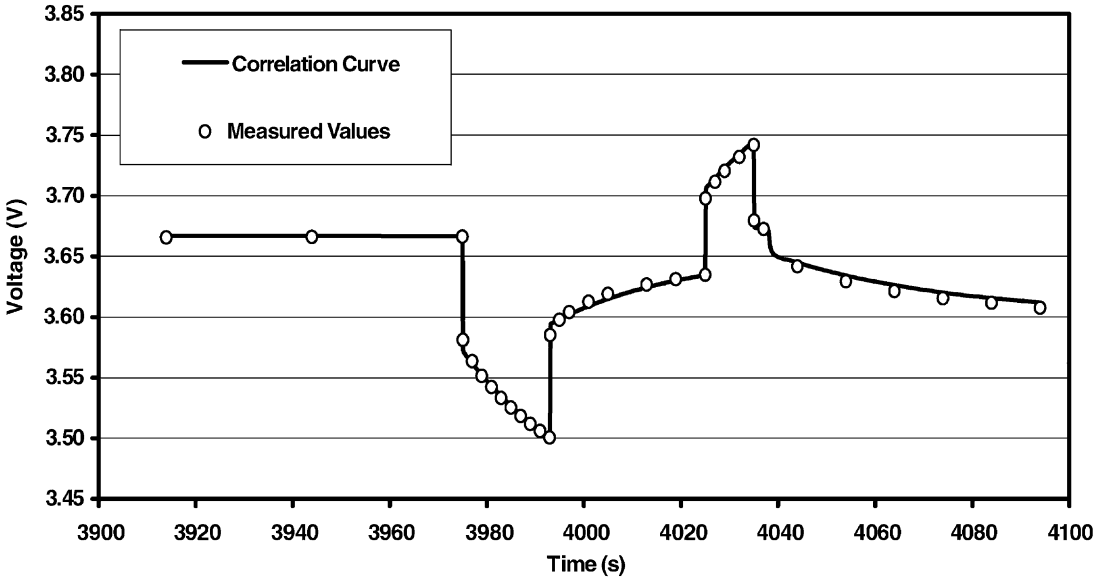


Fig. 3. Voltage data for HPPC test on Gen-2 18650 cell showing agreement between measured voltages and lumped-parameter battery model.

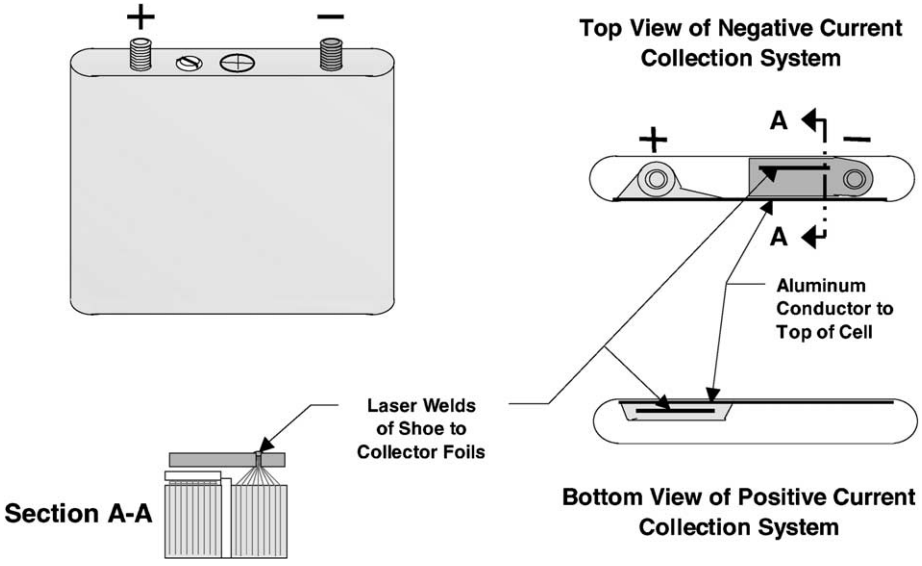


Fig. 4. Flat-wound lithium-ion cell design.

pass to a shoe or bracket that is attached to the terminal (Fig. 4). Both terminals are located on top of the cell. The aluminum shoe of the positive electrode at the bottom of the cell is connected to the terminal by an insulated aluminum conductor located between the cell winding and the cell enclosure. The aluminum top of the cell can be fastened to a deep drawn container by either crimping or welding.

The input parameters for the five batteries were identical except that the number of cell windings in the cells was increased for each succeeding battery to study the effect of this variable on the dimensions, weight, and performance of the batteries. Some of the parameters for the first, third, and fifth of these batteries are shown in Table 4. Input parameters for the batteries that were held constant were the battery power at the lower end of the SOC operating range, and the regeneration power at the top of the range. These parameters are set by the PNGV goals. Each of the batteries was designed with four 12-cell modules. The area of the cell electrodes and the capacity of the cells varied with the number of cell windings. The effect of changing the number of windings upon the cell thickness and capacity is shown in Fig. 5. To meet the set power for the battery, the program automatically adjusted the minimum voltage at maximum power and the maximum voltage at maximum regeneration

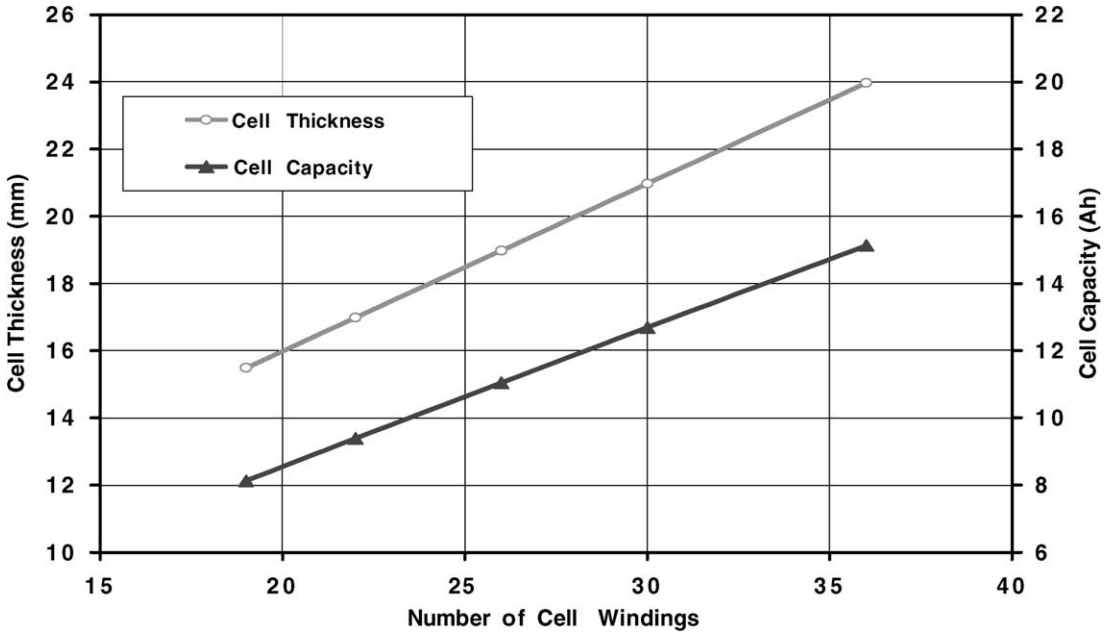


Fig. 5. Effect of number of cell windings on cell thickness and cell capacity, Gen-2 lithium-ion flat-wound cells, 100 mm cell width, 110 mm cell height.

Table 4
Batteries of flat-wound, Gen-2 lithium-ion cells designed for power-assist HEV, dielectric coolant

| Cell parameters | Battery 1 | Battery 3 | Battery 5 |
|---|---|---|---|
| Electrode thickness (μm) | | | |
| Negative electrode | 35 | 35 | 35 |
| Positive electrode | 35 | 35 | 35 |
| Number of cell windings | 19 | 26 | 36 |
| Height (mm) | 110 | 110 | 110 |
| Width (mm) | 100 | 100 | 100 |
| Thickness (mm) | 15 | 19 | 24 |
| ASI for 18 s power pulse (ohm $cm^2$) | 28.6 | 28.5 | 28.7 |
| Initial power (W) | 685 | 683 | 682 |
| Initial capacity (Ah) | 8.1 | 11.0 | 15.1 |
| Battery parameters | | | |
| Number of cells | 48 | 48 | 48 |
| Number of modules | 4 | 4 | 4 |
| Cooling fluid | Silicone | Silicone | Silicone |
| Power margin to allow for degradation (%) | 30 | 30 | 30 |
| Rated discharge power (kW) | 25 | 25 | 25 |
| Rated regeneration power (kW) | 30 | 30 | 30 |
| Minimum discharge voltage (V) | 118 | 139 | 151 |
| Maximum charge voltage (V) | 205 | 199 | 194 |
| Available energy (Wh) | 300 | 300 | 300 |
| Available capacity (% of rated capacity) | 21.2 | 15.6 | 11.4 |
| Values for lumped-parameter model (new battery) | | | |
| Ohmic resistance (48 cells ohms) | | | |
| Electrodes and separators | 0.106 | 0.078 | 0.057 |
| Cell current collection | 0.007 | 0.006 | 0.005 |
| Battery connectors | 0.005 | 0.005 | 0.005 |
| Total ohmic resistance | 0.118 | 0.089 | 0.067 |
| Polarization resistance (ohms) | 0.138 | 0.101 | 0.074 |
| Polarization time constant ($t$), (s) | 27 | 27 | 27 |
| Length (mm) | 428 | 512 | 631 |
| Width (mm) | 238 | 238 | 238 |
| Height (mm) | 151 | 151 | 151 |
| Volume (l) | 15 | 18 | 23 |
| Weight (kg) | 23 | 29 | 36 |
| Initial power density (kW/l) | 2.12 | 1.77 | 1.44 |

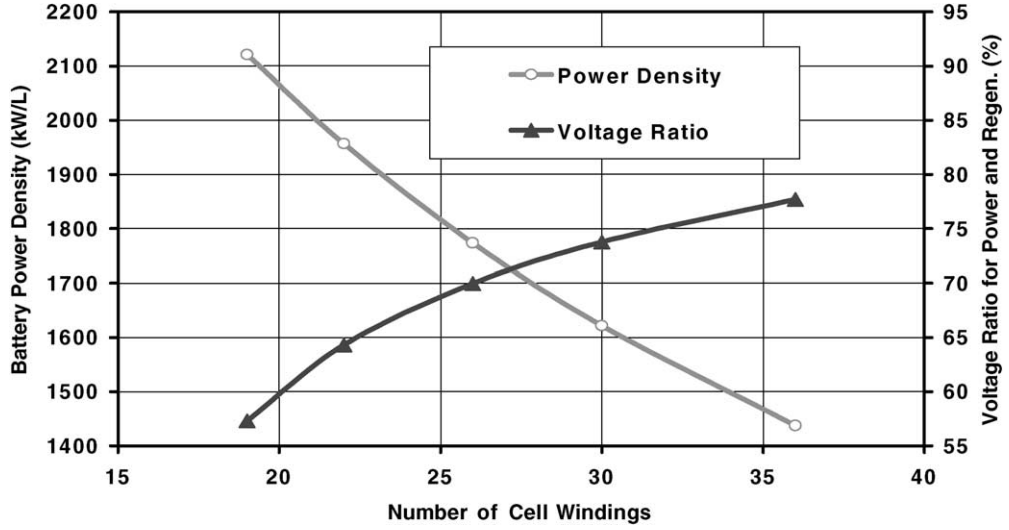


Fig. 6. Effect of number of cell windings on battery power density and ratio of battery voltages for full discharge power and regeneration power, using Gen-2 lithium-ion flat-wound cells, 100 mm cell width, 110 mm cell height.

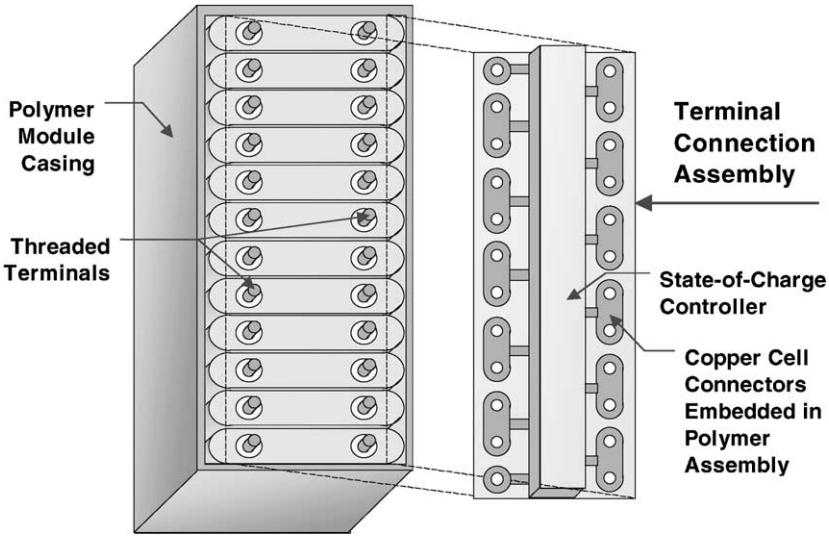


Fig. 7. Twelve-cell lithium-ion battery module for HEVs.

power. The program also adjusted the range of the state of charge over which the battery is operated to meet the available energy goal of 300 W. In determining the voltages at the maximum power and maximum regeneration power, the cell impedance's are calculated at the appropriate states of charge from equations determined for the values fit to the data of Fig. 2. The net effect of increasing the number of cell windings on the battery power density and upon the ratio of the voltage at full power to that at full regeneration power is shown in Fig. 6.

In addition to designing the cell, the program designs the module and the battery, calculates the weights and volume of the additional components, and calculates the additional resistance of the inter-cell connectors, battery terminals, and cables. It also designs the thermal control system, which is discussed in a companion paper [4]. The module (Fig. 7) contains twelve cells in series connection, which are interconnected with a pre-assembled unit that contains the cell interconnects embedded in a polymer and a SOC adjusting unit with built-in connections. Spacers provide a 1 mm-wide flow space between the cells. The batteries were designed to consist of four modules (48 cells total in series connection) with sufficient space for connections and flow passages and 12 mm-thick exterior insulated walls with 1 mm-thick aluminum sheet on the inside and outside surfaces.

## 4. Discussion of results

As discussed above, 30% excess power is provided for the battery design to allow for performance degradation during aging. Initially, the batteries described in Table 4 could provide 32.5 kW of power at the lowest state of charge in the operating range and for the minimum discharge voltage. Similarly, they could initially accept a charging rate of 39 kW at the top of the operating range. It is not expected that these high power values would be reached, but when the battery has degraded, the voltages might approach the values shown in generating the rated power values.

Although all of the batteries designed in this study have the same power under the prescribed conditions, they are not equal in other respects. Of the five batteries, Battery 1 has the least weight, volume, and cost. However, its small cell capacity and small electrode area result in the highest battery resistance and the lowest cell voltage (2.86 V initially and 2.48 V after battery degradation) at full battery power. This occasional low cell voltage may shorten the battery life. Battery 5 is at the other extreme, that is, it provides the power at a very high minimum cell voltage (3.28 and 3.16 V after battery degradation), but has the highest weight, volume, and cost of the batteries considered. The intermediate conditions provided by Battery 3 appear to be the best overall choice.

As noted above, the cell impedance's shown in Fig. 2 were used in designing the batteries and for calculating the maximum power on charge and discharge. However, the impedance's are valid only for the specific conditions under which they were measured, that is, for constant current discharge or charge for the specific duration of the measurements of 18 and 2 s, respectively. For any other conditions, such as for vehicle simulation studies, it is necessary to calculate the battery voltage by means of Eqs. (1) and (2), using battery values rather than cell values. The battery values for Eq. (2) are given in Table 4 and would be useful over the SOC range of approximately 35 to 60% where the parameters are relatively constant.

The shapes, volumes, and weights of the batteries all meet the PNGV requirements. Battery 3, which has favorable voltage and power density attributes, would have a volume of 18 l (versus a PNGV goal of 32 l) and a weight of 28 kg (versus a goal of 40 kg).

## 5. Conclusions

The test results for the 18650 cells provided an excellent basis for modeling full-scale batteries. The resistance of the current collection system for the 18650 cells was only a small fraction of the total cell impedance. When this resistance was subtracted from the total cell impedance, the impedance so obtained for the bare cell layers is believed to be a reliable basis for designing full-scale cells and batteries. In designing the full-scale batteries, the calculated resistance of the cell current collection system was added to the impedance of the basic cells to obtain the total impedance. The calculated impedance's for the batteries was extended to include the lumped-parameter model data and are believed to be sufficiently reliable for use in vehicle simulation studies.

Five batteries were designed for which the number of windings around the cell core was increased for each succeeding battery to study the effect of this variable upon the dimensions, weight, and performance of the batteries. All the batteries in the study were designed to meet precisely the PNGV goals for power and capacity, but the batteries with cells of fewest windings required the lowest voltage and highest currents to meet the power goal. The cells with the largest number of windings resulted in batteries of the highest weight and volume. Those of intermediate numbers of windings appeared to have the best overall performance.

## Acknowledgements

This work was supported by the US Department of Energy, Office of Advanced Automotive Technologies, under Contract No. W-31-109-Eng-38. Thanks also to Dennis Dees of Argonne National Laboratory for discussions on the modeling and review of the paper.

## References

[1] PNGV Battery Test Manual, Revision 3, DOE/ID-10597, February 2001.
[2] I. Bloom, J. Power Sources 101 (2001) 238–247.
[3] PNGV Battery Test Manual, Revision 3, Appendix D, DOE/ID-10597, February 2001.
[4] P. Nelson, K Amine, G. Henriksen, J. Power Sources 110 (2) (2002) 349–356.